07,18,19

Mechanical properties and thermal conductivity of composites based on crumpled graphene and nickel nanoparticles: molecular dynamics

© K.A. Krylova[1,2], L.R. Safina[1,¶], R.T. Murzaev[1], S.A. Shcherbinin[3,5], J.A. Baimova[1,4], R.R. Mulyukov[1,2]

[1] Institute for Metals Superplasticity Problems, Russian Academy of Sciences,
Ufa, Bashkortostan, Russia
[2] Ufa State Petroleum Technological University,
Ufa, Bashkortostan, Russia
[3] Peter the Great St. Petersburg Polytechnic University,
St. Petersburg, Russia
[4] Ufa University of Science and Technology,
Ufa, Bashkortostan, Russia
[5] Institute for Problems in Mechanical Engineering of the Russian Academy of Sciences,
St. Petersburg, Russia

¶ E-mail: saflia@mail.ru

Received June 5, 2023
Revised June 20, 2023
Accepted June 21, 2023

The mechanical properties and thermal conductivity of a composite based on crumpled graphene flakes and nickel nanoparticles obtained by high-temperature hydrostatic compression are investigated by the molecular dynamics. The pores of the graphene matrix of the composite are filled with nickel nanoparticles of different sizes (respectively, different contents of Ni — 8, 16 and 24 at.%). It was found that an increase in the amount of nickel on the one hand increases the thermal conductivity of the composite, and on the other hand reduces its strength, since strength is determined by the presence of a graphene network, and thermal conductivity is determined by the presence of a conductive metal. The obtained results on thermophysical properties combined with high mechanical characteristics of Ni/graphene composites allow us to predict their application for the manufacture of new flexible electronics, supercapacitors and lithium-ion batteries.

Keywords: crumpled graphene, Ni/graphene composite, mechanical properties, thermal conductivity coefficient, molecular dynamics.

DOI: 10.61011/PSS.2023.09.57118.101

1. Introduction

Currently, graphene and various materials based on carbon polymorphs are taking increasingly greater importance thanks to their unique properties. In particular, new types of composites based on graphene, nanotubes, nanodiamond particles, etc., are emerging [1–4]. Composites based on a graphene- reinforced metal matrix, where Al, Ni, Mg, Zn, Cu and Ti or their alloys are used as a matrix, are one of the important research areas. Thanks to the properties of graphene such as flexibility, high strength and light weight, it is useful for virtually all industrial applications. Taking into account its outstanding mechanical properties, graphene has been an important reinforcing element for production of composites over the last years [5–8]. For example, ultimate tensile strength of Al/graphene composite has increased by 62% compared with that of pure aluminium [5]. Addition of graphene to the metal matrix may influence to a great extent also other properties of the final composite. Investigations of metal matrix composites, where graphene was used as a reinforcing material, are reviewed in [8].

Composites based on graphene network and metal nanoparticles are another newer research area [9–12]. In such composite morphology, graphene network is responsible for strength, while the metal filling is responsible for the change of other properties such as conductivity. Such new morphology can be achieved thanks to the ability of graphene to „wrap“ nanoparticles forming strong capsules with metal inside them [10]. By now, we have trialed various techniques for composite production from various metal nanoparticles [10–12]. Thanks to their unique properties,they can be used as reinforcing coatings to produce new lithium-ion batteries and supercapacitors.

Graphene network features the following specifications: (1) high electrical conductivity compared with graphite carbon; (2) large surface area; (3) high surface-volume ratio ensuring more active centers for adsorption; (4) high flexibility that is important for flexible electronics; (5) thermal and chemical resistance. Moreover, such material made using chemical delamination of graphite may be manufactured commercially with relatively low cost that is important for its application.

One of suitable metals to be used for filling crumpled graphene pores are Ni nanoparticles. Nickel has high corrosion resistance, high elasticity and ductility, and is a good catalyst, etc. In addition, the fact that rather strong bond

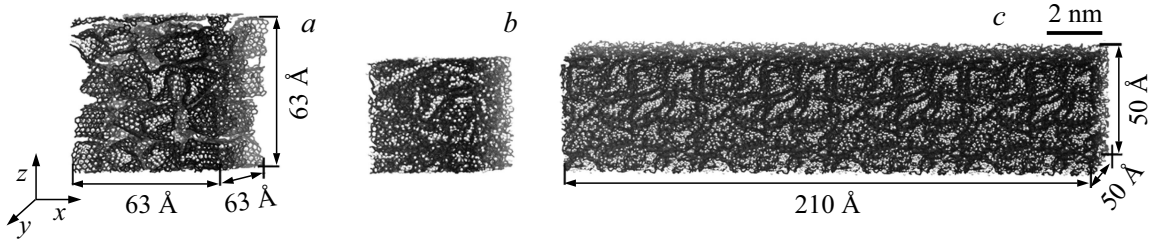

Figure 1. (*a*) Initial structure of the Ni/graphene composite. (*b*) Composite structure after hydrostatic compression at $T = 1000$ K. (*c*) Scaled up composite structure for thermal conductivity calculation. Ni atoms are grey, and carbon atoms are black.

between Ni and graphene prevails at the interface makes the choice of this metal more preferable [17]. Therefore, Ni is widely used as a metal substrate for growing graphene and carbon nanotubes [18]. Investigation of mechanical and physical properties of a composite based on crumpled graphene and Ni nanoparticles is of great interest, thus, addition of Ni to crumpled graphene may considerably improve both mechanical and physical properties of the future material.

Experimental work on new composite morphologies is supported by extensive theoretical research using *ab initio* or molecular dynamics (MD) calculations for better understanding of the mechanisms behind the improvement of material properties [4,13–16,19–21]. For example, [14] shows that discrete graphene sheets covering Ni particles are collected into an intact and continuous graphene network when treated by sintering. Graphene flakes are mixed with Ni matric forming an interlinked structure. Simulation shows that addition of graphene sheets may efficiently block dislocation propagation [16], while the increase in the graphene layer length allows to avoid initiation of dislocations at the graphene sheet end and increases the structural strength.

Therefore, the molecular dynamics is used herein to investigate the mechanical properties and thermal conductivity of composites based on carbon matrix (crumpled graphene) and metal nanoparticles (Ni). The effect of the number of metal atoms on the composite strength and thermal conductivity has been analyzed. It has been shown that mechanical and thermal properties of composites may be controlled by varying composite morphology.

2. Simulation details

The initial structure is crumpled graphene (porous material consisting of folded graphene flakes interconnected with each other by Van der Waals forces) filled with Ni nanoparticles. Three composite structures containing Ni: 8, 16 and 24 at.% are addressed herein. Hereinafter for clarity, the composite structure containing Ni 8 at.% will be referred to as CG8, containing Ni 16 at.% — as CG16, and containing Ni 24 at.% — as CG24, and the crumpled graphene structure without Ni nanoparticles will be referred to as CG. Figure 1, *a* shows the initial structure of the Ni/graphene composite precursor: crumpled graphene flakes (black) filled with Ni nanoparticles (grey). It is known that edge atoms of the graphene flakes have *sp*-hybridization and can easily form new bonds with adjacent graphene flakes or with other elements, for example, hydrogen, oxygen, nitrogen and various functional groups. For clarity, pure crumpled graphene without the influence of other element atoms will be addressed herein. More detailed methodology for obtaining the initial structure is described in [22,23].

Earlier, [22–24] have shown that metal/graphene composites may be successfully produced by high-temperature hydrostatic compression. Therefore, the design simulation cell is subjected to strain-controlled hydrostatic compression ($\varepsilon_x = \varepsilon_y = \varepsilon_z = \varepsilon$) at a rate of $0.01\,\text{ps}^{-1}$ until the maximum density is achieved: $\rho_{CG8} = 5.28$, $\rho_{CG16} = 6.54$, $\rho_{CG24} = 7.80\,\text{g/cm}^3$. Compression is performed at 1000 K, i. e. $T = 0.6{-}0.8T_{\text{melt}}$, where T_{melt} is the melting temperature of a Ni nanoparticle with the chosen size. It should be noted that the melting temperature of Ni nanoparticles is about 1360 K [25], and the graphene melting temperature is 5000 K [26]. The structure after hydrostatic compression is shown in Figure 1, *b*. The final dimensions of the Ni/graphene composite are about $43 \times 43 \times 43$ Å with a density of $5.15\,\text{g/cm}^3$. This structure is used to calculate mechanical properties of the composite.

Various methods used to estimate the mechanical properties of the Ni/graphene composites are described in detail in [27]. One of the methods involves step-by-step deformation, where each of n tension steps are followed by m structure relaxation steps. Another uniaxial tension method includes dynamic deformation, which is applied continuously at a constant rate. The study will estimate the mechanical properties of the Ni/graphene composite using the second deformation method — dynamic tension.

Figure 1, *c* shows the initial structure used to calculate thermal conductivity of the composite. First, the composite structure was subjected to relaxation to achieve thermodynamic equilibrium at temperatures from 100 to 600 K with increment 100 K. For this, first, NPT assembly and then NVE assembly were used (each of them was used during 1 ps).

Thermal conductivity of the composite is compared with that of $205 \times 51 \times 51$ Å pure single-crystal Ni. The x, y and z axes coincide with crystallographic directions [100],

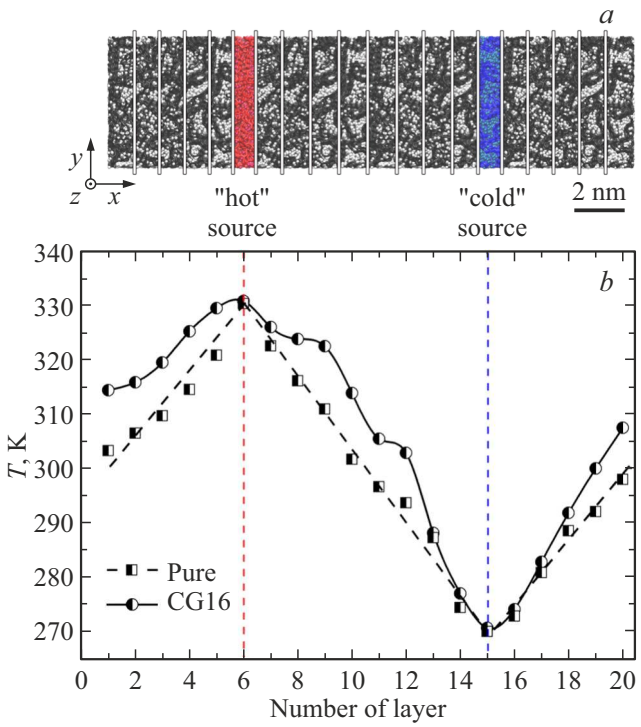

Figure 2. (a) Ni/graphene composite separated into 20 regions for calculation. Red and blue region correspond to the „hot“ and „cold“ sources. Carbon and nickel atoms are black and grey, respectively. (b) Temperature profile by layers for pure Ni and CG16 composite after exposure at 300 K. Dots show design values, dashed line is the linear approximation of design data.

[010] and [001], respectively. Relaxation of Ni samples is carried out in the same conditions as for the composite structure.

After achievement of the thermodynamic equilibrium, the design cell is split along the long side into 20 equal regions with a width of 10−10.5 Å, as shown in Figure 2, a. Here, the heat source is the sixth (red) region and the heat sink is the fifteenth (blue) region. Between the „hot“ and „cold“ sources, a temperature gradient is set on the structure length resulting in the occurrence of a heat flux ΔQ. Temperatures of the „hot“ and „cold“ regions are equal to $T + \Delta T$ and $T - \Delta T$, respectively. ΔT is 10% of the system temperature. The temperature of other regions at the start of simulation is T, with six different temperatures $T = \{100, 200, 300, 400, 500, 600\}$ K used for the calculation. For each state, three to five thermal conductivity measurements are performed. Standard deviation of these values varied within 5−7% at each temperature.

As an example, Figure 2, b shows temperature distribution across the simulation cell for pure Ni and CG16 composite after exposure at 300 K. Note that for other composites, temperature profiles are close. The mean temperatures of „cold“ and „hot“ thermostat are 270 and 330 K, respectively. The mean temperature is also calculated in other regions. Note that for pure Ni, the temperature profile has typical linear behavior (black dashed line in Figure 2, b). For metals, heat transfer is more uniform than for Ni/graphene composites with high covalent bond and complex crystal structure. Temperature profiles of composites with Ni nanoparticles (Figure 2, b) are nonlinear.

LAMMPS software suite is used for simulation. To describe interatomic interactions in the Ni/graphene system, three potentials are used: AIREBO (describes C−C interaction) [28], Morse (describes C−Ni interaction) [29,30] and EAM (embedded atom method used to describe Ni−Ni interaction) [31]. Efficiency of AIREBO, Morse and EAM potentials for solution of problems addressed herein is confirmed in [31–34]. For visualization of the structure, VMD (Visual Molecular Dynamics) software is used to display and analyze structural changes at particular simulation stages [35].

3. Findings and discussion

3.1. Mechanical properties

Figure 3, a shows stress-strain curves in uniaxial tension. It is shown that the mechanical properties of CG8 composite are the highest and are close to the strength of pure crumpled graphene, in particular, with strain $\varepsilon_{xx} > 1.2$. CG24 composite has the lowest strength. This confirms that graphene network is responsible for composite strength and the presence of metal makes the strength lower. For all three Ni/graphene composites, Young's moduli were calculated: 249 GPa, 245 GPa and 230 GPa for CG8, CG16 and CG24, respectively. Note that the Young's modulus of the crumpled graphene without atoms is equal to 330 GPa.

Maximum tensile strengths for CG8, CG16 and CG24, respectively, are equal to 125 GPa, 107 GPa and 87 GPa. Such high stresses in the Ni/graphene composite may be explained by formation of a strong graphene network. However, Figure 3, a shows that the ultimate strain, when structures failure occurs, is not achieved. Nanoparticle size has a high influence on the mechanical properties of composites. The lower the Ni nanoparticle size, the easier new chemical bonds between adjacent structural members of composites occur, and therefore, the higher composite strength.

Figures 3, b and c show Ni nanoparticle distribution in uniaxial tension in composites with the lowest (CG8) and the highest (CG24) content of Ni. Note that carbon atoms are not shown. It is apparent that in the initial composite structure, Ni atom distribution is more uniform in CG8 structure than in CG24 structure. Ni nanoparticles in CG24 structure are consolidated and have sufficiently large size. In CG8, Ni atoms are distributed across the carbon network and have no the nanoparticle shape any more (see Figure 3, b). Therefore, the strength of such composite achieves the values typical for the crumpled graphene strength at $\varepsilon_{xx} > 1.2$. Appearance of new chemical bonds during hydrostatic compression in the structure with large nanoparticles is rather complicated, because all

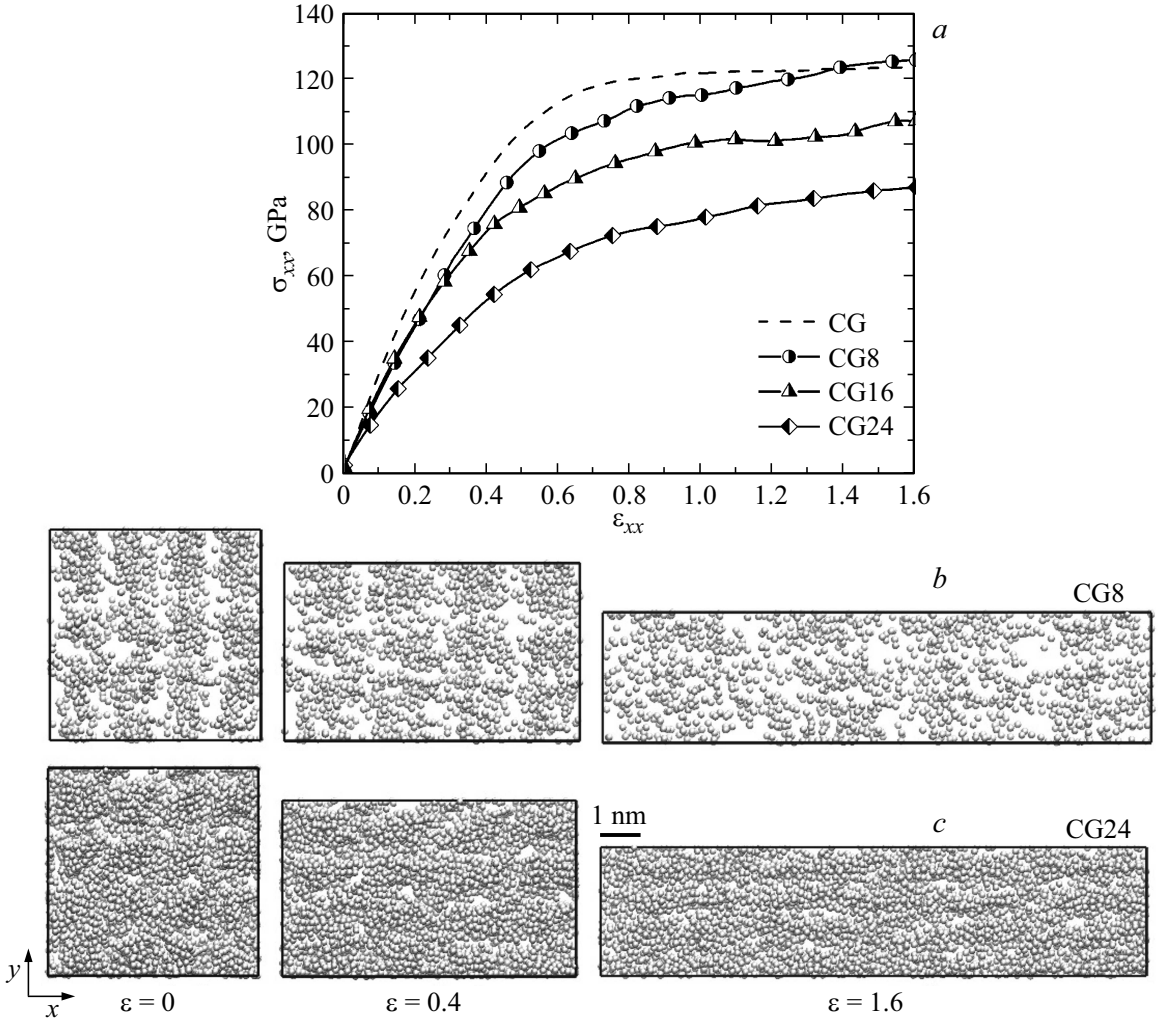

Figure 3. (*a*) Stress-strain curves in the uniaxial tension for Ni/graphene composite with various Ni content (dots and solid lines) and for crumpled graphene (CG, dashed line). (*b, c*) Ni nanoparticle distribution in the CG8 and CG24 structures with various degrees of strain in uniaxial tension. Carbon atoms are not shown.

carbon atoms have been already involved in the interaction with Ni nanoparticles, thus, reducing the strength of such composites.

3.2. Thermal conductivity coefficient

Dependence of the thermal conductivity coefficient on temperature (λ) for all composites studied herein is shown in Figure 4. Thermal conductivity of Ni/graphene composite depends on the Ni concentration: the higher Ni concentration, the higher thermal conductivity at all temperatures. Decrease of λ with increasing graphene concentration is also shown for Cu/graphene composites [36].

However, thermal conductivity of Ni/graphene composites depends on temperature very slightly, and the existing variation of the thermal conductivity coefficient with growing temperature is associated with the emerging new contact interfaces between Ni and graphene. Note that the obtained thermal conductivity at 100−200 K may be underestimated due to the features of MD simulation that takes into account only phonon (lattice) thermal conductivity and does not take into account the electronic thermal conductivity. For metals and alloys, the effect of the electronic thermal conductivity is low at $T < 100$ K. However, for Ni/graphene composites, the electronic thermal conductivity may make a significant contribution to the system thermal conductivity even at $T > 100$ K.

For pure single-crystal Ni (black squares in Figure 4), λ values are comparable with the experimental curve typical for bulk polycristalline Ni [37] (black dashed curve in Figure 4). The observed decrease of λ at $T < 500$ K is attributable to the dimensions of the test samples. It is shown in [38] that small Ni nanoparticles have lower thermal conductivity than bulk nickel. And with increasing nanoparticle size, thermal conductivity increased approaching $\lambda_{\text{bulk}} = 91$ W/(mK) (thermal conductivity of bulk polycrystalline Ni at 300 K [37]). Increase in the Ni nanofilm thickness also results in the increase in λ at 300 K

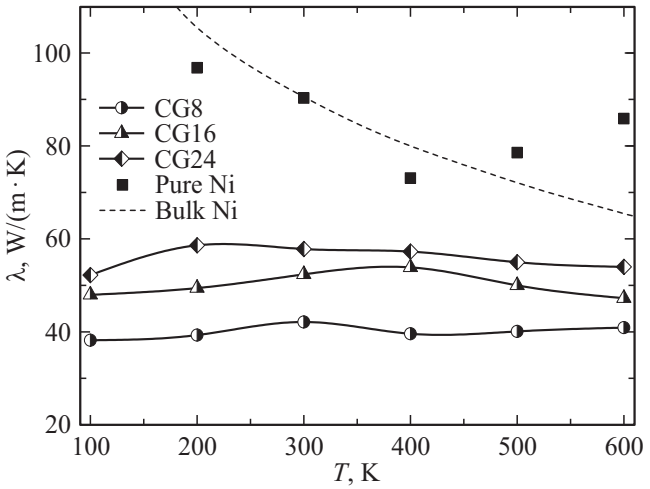

Figure 4. Thermal conductivity of pure Ni and Ni/graphene composite depending on temperature. Dashed line shows the experimental data for bulk polycrystalline Ni [35] and squares show λ of pure single-crystal Ni determined herein.

to the values typical for bulk Ni [39]. Thermal conductivity at 500 K and 600 K is even higher than that of bulk Ni. This may be explained by melting or partial melting of Ni nanoparticles during simulation. Since the particle size is small, then their melting temperature may be much lower than the melting temperature of bulk Ni [40].

Control of thermal properties using various internal and external factors is of key importance [41]. It is shown herein that variation of Ni concentration allows to control thermal conductivity of composites: increasing Ni concentration in the composite results in increasing thermal conductivity of the system (Figure 4). However, λ for CG16 and CG24 composites has close values.

Thermal conductivity of the Ni/graphene composite may be affected by several factors. For example, small size of graphene flakes in the composite structure limits the thermal conductivity [42] like the addition of Ni atoms. The latter transform carbon atoms with sp^2-hybridization into atoms with sp^3-hybridization resulting in the failure of the ideal π-electron-coupled structure. Phonon (main heat carriers) scattering over defects and graphene fold apexes may also reduce thermal conductivity as well as the appearance of new bonds between graphene flakes and, thus, reduce heat exchange.

4. Conclusion

Molecular dynamic method was used to investigate strain behavior, strength and thermal conductivity of Ni/graphene. It is shown that mechanical and thermal properties of composite have high dependence on the concentration of Ni.

In uniaxial tension, the ultimate strength of the Ni/graphene composites is lower, when the number of Ni atoms in the structure is higher. CG8 composite, whose ultimate strength reaches the values typical for crumpled graphene, has the highest strength. Such high strength in this composite is associated with Ni atom distribution across the graphene network resulting in formation of new chemical bonds between graphene flakes. In other composite structures, such Ni atom distribution is not observed, nanoparticles retain their integrity and, therefore, formation of new carbon bonds is hindered. This results in reduced strength of CG16 and CG24 composites compared with crumpled graphene and CG8 composite.

Thermal conductivity of the Ni/graphene composite is much lower than that of pure Ni (91 W/(mK) [37]), but is much higher than that of crumpled graphene (2.183 W/(mK) [43]). Formation of a highly deformed structure of crumpled graphene during its fabrication results in formation of folds that reduce thermal conductivity of the structure. Increasing number of Ni atoms in the composite results in increasing thermal conductivity due to addition of an element with higher thermal conductivity. Formation of new contact boundaries between the nickel and carbon phases also has a great impact on the thermal conductivity of the composite. Moreover, thermal conductivity of the Ni/graphene may be controlled by varying Ni concentration. It should be noted that addition of Ni to crumpled graphene results in increasing thermal expansion, and the higher Ni concentration, the higher thermal expansion coefficient [44]. However, increasing temperature almost does not influence the thermal conductivity coefficient of composites, though for pure Ni, significant decrease of thermal conductivity coefficient is observed with temperature growth.

Mechanical properties of composite are greatly affected by the presence of graphene network, and the higher nickel concentration, the lower composite strength. The thermal conductivity coefficient is greatly affected by the presence of conducting metal — the higher the number of Ni atoms, the higher system thermal conductivity.

The achieved combination of high mechanical properties with controlled thermal properties facilitates potential utilization of the Ni/graphene composites as alternative materials in various industrial application. For example, such composites can be currently used as chemical sensors, energy or hydrogen accumulators, in batteries and supercapacitors [45,46].

Acknowledgments

The authors acknowledge Peter the Great Saint-Petersburg Polytechnic University Supercomputer Center „Polytechnic“ for computational resources.

Funding

The work of K.A. Krylova, L.R. Safina, R.T. Murzaev, J.A. Baimova was supported by the grant of the Russian Science Foundation (No. 20-72-10112). The work of R.R. Mulyukova was supported by the State Assignment of IMSP RAS. The work of S.A. Shcherbin was supported

financially by the Ministry of Science and Higher Education of the Russian Federation (job-order 0784-2020-0021).

Conflict of interest

The authors declare that they have no conflict of interest.

References

[1] M.M. Slepchenkov, P.V. Barkov, O.E. Glukhova. ZhTF **93**, *4*, 481 (2023).
[2] M.K. Rabchinskii, A.D. Trofimuk, A.V. Shvidchenko, M.V. Baidakova, S.I. Pavlov, D.A. Kirilenko, Yu.V. Kulvelis, M.V. Gudkov, K.A. Shiyanova, V.S. Koval, G.S. Peters, V.T. Lebedev, V.P. Melnikov, A.T. Dideikin, P.N. Brunkov. Tech. Phys. **67**, *12*, 1611 (2022).
[3] A.G. Sheinerman, S.A. Krasnitskii. Tech. Phys. Lett. **47**, *12*, 873 (2021).
[4] J.A. Baimova, S.A. Shcherbinin. Materials **16**, *1*, 202 (2023).
[5] J. Wang, Z. Li, G. Fan, H. Pan, Z. Chen, D. Zhang. Scripta Mater. **66**, 594 (2012).
[6] A.A. Leonov, E.V. Abdulmenova, M.A. Rudmin, J. Li. Lett. Mater. **11**, *4*, 452 (2021).
[7] O.Y. Kurapova, I.V. Smirnov, E.N. Solovyeva, I.Y. Archakov, V.G. Konakov. Lett. Mater. **10**, *2*, 164 (2020).
[8] Ö. Güler, N. Bağcı. J. Mater. Res. Technol. **9**, *3*, 6808 (2020).
[9] I.A. Zavidovskiy, A.A. Khaidarov, O.A. Streletskiy. Phys. Solid State **64**, *8*, 474 (2022).
[10] D. Wei, J. Liang, Y. Zhu, Z. Yuan, N. Li, Y. Qian. Part. Part. Syst. Char. **30**, *2*, 143 (2013).
[11] X. Li, J. Natsuki, T. Natsuki. Physica E **124**, 114249 (2020).
[12] Z.-S. Wu, G. Zhou, L.-C. Yin, W. Ren, F. Li, H.-M. Cheng. Nano Energy **1**, *1*, 107 (2012).
[13] C. Qiu, Y. Su, J. Yang, B. Chen, Q. Ouyang, D. Zhang. Compos. C **4**, 100120 (2021).
[14] Y. Yang, M. Liu, J. Du, W. Zhang, S. Zhou, W. Ren, Q. Zhou, L. Shi. Carbon **191**, 55 (2022).
[15] D. Rapp, S. Hocker, H. Lipp, S. Schmauder. Comput. Mater. Sci. **226**, 112247 (2023).
[16] Y. Huang, Z. Yang, Z. Lu. Comp. Mater. Sci. **186**, 109969 (2021).
[17] M. Yang, Y. Liu, T. Fan, D. Zhang. Prog. Mater. Sci. **110**, 100652 (2020).
[18] N.-W. Pu, G.-N. Shi, Y.-M. Liu, X. Sun, J.-K. Chang, C.-L. Sun, M.-D. Ger, C.-Y. Chen, P.-C. Wang, Y.-Y. Peng, C.-H. Wu, S. Lawes. J. Power Sources **282**, 248 (2015).
[19] A.Y. Galashev, O.R. Rakhmanova. Phys. Lett. A **384**, *31*, 126790 (2020).
[20] A.E. Galashev, L.A. Elshina, R.V. Muradymov. Russ. J. Phys. Chem. A **90**, 2444 (2016).
[21] A.E. Galashev, O.R. Rakhmanova, L.A. Elshina. Russ. J. Phys. Chem. B **12**, *3*, 403 (2018).
[22] L.R. Safina, J.A. Baimova, K.A. Krylova, R.T. Murzaev, S.S. Shcherbinin, R.R. Mulyukov. Phys. Status Solidi RRL **15**, *1*, 2100429 (2021).
[23] L.R. Safina, K.A. Krylova, J.A. Baimova. Mater. Today Phys. **28**, 100851 (2022).
[24] Y. Zhang, F.M. Heim, J.L. Bartlett, N. Song, D. Isheim, X. Li. Sci. Adv. **5**, *5*, 1 (2019).
[25] L.R. Safina, J.A. Baimova, R.R. Mulyukov. Mech. Adv. Mater. Mod. Proc. **5**, 2 (2019).
[26] E. Ganz, A.B. Ganz, L.-M. Yang, M. Dornfelda. Phys. Chem. Chem. Phys. **19**, 3756 (2017).
[27] K.A. Krylova, L.R. Safina, S.A. Shcherbinin, J.A. Baimova. Materials **15**, *11*, 4038 (2022).
[28] S.J. Stuart, A.B. Tutein, J.A. Harrison. J. Chem. Phys. **112**, *14*, 6472 (2000).
[29] K.P. Katin, V.S. Prudkovskiy, M.M. Maslov. Micro Nano Lett. **13**, *2*, 160 (2018).
[30] A.Y. Galashev, K.P. Katin, M.M. Maslov. Phys. Lett. A **383**, *2–3*, 252 (2019).
[31] M.I. Mendelev, M.J. Kramer, S.G. Hao, K.M. Ho, C.Z. Wang. Phil. Mag. **92**, *35*, 4454 (2012).
[32] C. de Tomas, I. Suarez-Martinez, N.A. Marks. Carbon **109**, 681 (2016).
[33] V.E. Zalizniak, O.A. Zolotov. Mol. Simulat. **43**, *17*, 1 (2017).
[34] L.R. Safina, E.A. Rozhnova, R.T. Murzaev, J.A. Baimova. Appl. Sci. **13**, *2*, 916 (2023).
[35] W. Humphrey, A. Dalke, K. Schulten. J. Mol. Graphics **14**, *1*, 33 (1996).
[36] T. Wejrzanowski, M. Grybczuk, M. Chmielewski, K. Pietrzak, K.J. Kurzydlowski, A. Strojny-Nedza. Mater. Design **99**, 163 (2016).
[37] C.Y. Ho, R.W. Powell, P.E. Liley. Thermal Conductivity of Selected Materials. U.S. Department of Commerce, National Bureau of Standards, Washington (1968). 180 p.
[38] S.P. Yuan, P.X. Jiang. Int. J. Thermophys **27**, 581 (2006).
[39] A.A. Le-Zakharov, A.M. Krivtsov, A.V. Porubov. Continuum Mech. Therm. **31**, 1873 (2019).
[40] A.V. Verkhovtsev, S. Schramm, A.V. Solov'yov. Eur. Phys. J. D **68**, 246 (2014).
[41] A.V. Savin, O.V. Gendelman. Phys. Rev. E **89**, 012134 (2014).
[42] Z. Fan, A. Marconnet, S.T. Nguyen, C.Y. Lim, H.M. Duong. Int. J. Heat Mass Tran. **76**, 122 (2014).
[43] Y. Zhong, M. Zhou, F. Huang, T. Lin, D. Wan. Solar Energy Mater. Solar C **113**, 195 (2013).
[44] R.T. Murzaev, K.A. Krylova, J.A. Baimova. Materials 16, 3747 (2023).
[45] L. Cao, C. Wang, Y. Huang. Chem. Eng. J. **454**, 140094 (2023).
[46] T. Zhang, X. Gao, J. Li, L. Xiao, H. Gao, F. Zhao, H. Ma. Defence Technology (2023). In press

Translated by E.Ilyinskaya